

Research Paper

A Prognostic Approach to the Resonance Failure Problem by Triple Sensing Technology

Salih Seçkin EROL

*Center for Advanced Life Cycle Engineering
University of Maryland*

College Park, MD 20742 USA; e-mail: sserol@umd.edu

(received December 14, 2018; accepted September 17, 2019)

Within this study, resonance phenomenon, which is one of the crucial problems in mechanical constructions, has been analyzed with respect to oil starvation failure in a ball bearing. A unique test rig is designed, constructed, and placed in a laboratory ambience. A ball bearing on the electrical motor, which is a component of the test rig, has been selected for acquisition of data within triple sensing technology in vibration, acoustic, and electrical consumption through testing conditions. The target of that study is condition monitoring of oil starvation fault and resonance fault for comparison of various predictive maintenance methods. The testing was carried out within the electrical frequency of 40.5 Hz, which actuated the electrical motor in order to identify the rotation speed. According to the analyzed results, oil starvation fault and resonance fault is most accurately inspected by vibration analysis.

Keywords: oil starving; resonance; vibration; acoustic; electrical consumption.

1. Introduction

Mechanical systems require maintenance due to failures occurring or going to occur. Main maintenance methods implemented in manufacturing enterprises are breakdown approach, periodic approach, and predictive approach. Technique of predictive maintenance is based on collecting symptomatic data about health of the machine. Technical analysis approaches of the predictive maintenance are such as vibration, acoustics, heat, lubrication, electrical consumption, etc., consisting of the data characterizing the machine health. Resonance failure is one of the major problems for mechanical constructions. and oil starvation is a crucial factor for eliminating the resonance failure. In this study, effect of oil starvation on resonance failure is studied by means of comparison of acoustics technique, vibration technique, and electrical consumption. Evaluations are presented.

Maintenance is a crucial activity for maintaining minimal time loss and cost in manufacturing. Maximum performance and safety are the main purposes for industrial enterprises. A proactive approach in mechanical maintenance has been brought by the concepts of condition based maintenance and prognostics health management (CBM/PHM) that as-

sists with sustainable scheduled maintenance activities (LOUKOPOULOS *et al.*, 2019). Condition based maintenance that aims for asset health has been implemented successfully in many industries and consists of mainly three stages as monitoring, prognostics, and diagnostics (AYO-IMORU, CILLIERS, 2018). Breakdown maintenance requires unplanned stoppages and these stoppages are one of the reasons for high production losses and high economical costs due to repairing, renewing elements of the machine (COLLACOTT, 1977).

Beginner level cracked or broken rotor bars, small bearing damages, and axial misalignments may cause increase in the electrical current consumption (VELARDE-SUAREZ *et al.*, 2006). Time/resistance, temperature, acoustic emissions (HARDMAN *et al.*, 2000), and ultrasonic inspection, electrical current density changes take place in wide implementations as well. Traditional signal processing techniques are used in evaluating these parameters and consequently prognostic approach has been limited mainly to that area (ACOSTA *et al.*, 2006). Failures of the machines that have rotating elements are mainly caused by vibrational symptoms and are evaluated mostly by means of vibrational analysis (GOODENOW *et al.*, 2000).

WELZ *et al.* (2017) stated in their report that accuracy of the diagnostic model depends on new generic

predictive techniques with more integrated ambient maintenance activity information rather than classic approaches.

ER and TAN (2018) made a research on ensuring the quality of the unit product and preventing unexpected time loss during the planned maintenance. They studied experimental modal analysis and a frequency response function together for analyzing vibrations from machine components with the radial basis function approach for modelling cumulative vibration sensitivities.

2. Materials and methods

The experimental rig is designed as the combination of a frequency inverter, an AC induction motor, a double inlet fan and a flexible coupling. The tested rig is placed on a steel sheet and foundation. The tested rig is screwed to a double-decker rubber sheet placed on the tested rig and foundation; vacuum rubbers are placed under feet of the foundation stands on the floor. This test rig design within a data acquisition card and a triphase electrical motor are coupled for monitoring on a computer.

Theoretical (T) and practical (P) frequencies are represented in Table 1. Theoretical frequency (T) represents the one selected on frequency inverter; and practical frequency (P) is identified empirically. A frequency range gets some losses and consequently practical frequencies deviate. 1× accepted as the base frequency; while 2×, 3× and the higher multiplies are harmonics of the base frequency (EROL, 2016). Table 1 shows frequencies represented within the mark of *f* for frequency inverter and harmonic orders are given within abbreviation of *h*.

All the measurements were done over the tests in the electrical frequency of 40.5 Hz and rotation speed is detected as 2350 min⁻¹. Harmonics and failure frequencies are taken into account when calculating bearing and fan sourced vibration signals of the tested rig.

Bearing related formulations with basic failure frequency estimations and relevant measured values are presented in Table 2.

The formulas related to the failure frequencies of the bearing components are given in the Eqs (1)–(4):

$$\omega_{bpfo} = \omega_s \left(\frac{n}{2} \right) \left[1 - \frac{r}{d} \cos \phi \right], \tag{1}$$

$$\omega_{bpf_i} = \omega_s \left(\frac{n}{2} \right) \left[1 + \frac{r}{d} \cos \phi \right], \tag{2}$$

$$\omega_{bsf} = \omega_s \left(\frac{d}{2r} \right) \left[1 - \left(\frac{r}{d} \cos \phi \right)^2 \right], \tag{3}$$

$$\omega_c = \frac{\omega_s}{2} \left[1 - \frac{r}{d} \cos \phi \right], \tag{4}$$

where ω_{bpfo} is the outer ring passing frequency [Hz], ω_{bpf_i} is the inner ring passing frequency [Hz], ω_{bsf} is the ball spin frequency [Hz], ω_c is the cage frequency [Hz], ω_s is the shaft frequency [Hz], ω_{bpf} is the fan blade passing frequency [Hz], *n* is the number of balls, *r* is the diameter of ball, ϕ is the angle of contact, *d* is the diameter of division circle.

For checking the oil starvation fault, oil is completely removed through specified bearing; in order to manage fast deterioration, 0.55 g of oil has been applied on the bearing.

For evaluation of the measurements, the raw data referring to the vibration and acoustics techniques are investigated with the help of FFT (Fast Fourier Transform) approach and relevant data are processed in further steps. The data about electrical consumption have been identified according to the software algorithm of the device and further process has been based on PSD (Power Spectrum Density) and trending approach.

3. The experiment

Vibrational data were captured in radial and axial directions during tested conditions. Acoustic data are captured omni-directionally on the test rig covered by a plexyglass cabin. Vibration and acoustic signals are acquired with accelerometers coupled to a DAQ (Data Acquisition Card) and analyzed through the software

Table 1. Theoretical and practical frequencies.

<i>(f)</i>	<i>(h)</i>									
	1×		2×		3×		4×		5×	
	T	P	T	P	T	P	T	P	T	P
40.5	40.5	39.06	81	78.12	121.5	117.18	162	156.24	202.5	241.56

Table 2. Fault frequencies.

<i>f</i> [Hz]	ω_s [Hz]	ω_{bpf} [Hz]	ω_c [Hz]	ω_{bpfo} [Hz]	ω_{bpf_i} [Hz]	ω_{bsf} [Hz]
40.5	39.06	390.6	14.84	118.74	193.76	76.69

developed by the card manufacturer. Identifying natural frequencies for the analysis are determined by tests of damping which are implemented on the test rig during the mechanical construction but not through the dynamic behavior. Relevant data about electrical consumption have been acquired with a device coupled over an electrical circuit of the motor and its software is based on processing the acquired data.

3.1. Acoustic analysis

The highest five acoustic signal peaks are presented in Fig. 1, they are rooted through shaft rotation and bearing components. The base rotational frequency is 39.06 Hz and the largest magnitude is captured at $0.5 \times$ (19.53 Hz). Another order of the base frequency is captured at 312.5 Hz ($8 \times$) which is the second strongest magnitude in the frequency domain.

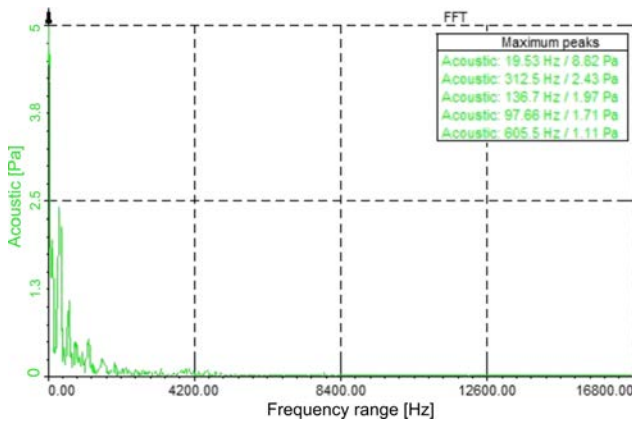


Fig. 1. Spectrum of acoustic data.

According to the Fig. 1, resonance cases are detected at frequencies of 136.7 Hz (third dominant), 97.66 Hz (fourth dominant), and 605.5 Hz (fifth dominant).

3.2. Vibration analysis

Five highest peaks of vibration signals in the axial direction are given in Fig. 2. The fundamental frequency at 39.06 Hz has been explored as the second signal in dominance within the amplitude of 0.326 m/s^2 . Harmonic on $1 \times$ that is the sign of lack of balance is found as the second dominant peak in the axial location. Vibration magnitude at 117.18 Hz ($3 \times$) forced the natural frequency signal at 120.8 Hz and superharmonic resonance occurred within the highest magnitude of 0.511 m/s^2 . Vibration in the harmonic belongs

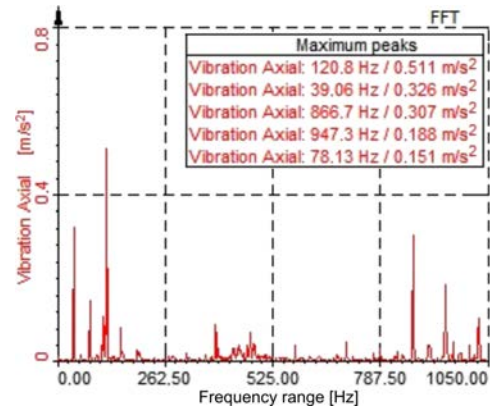


Fig. 2. Spectral view in vibration frequencies (axial direction).

to the cage frequency of 949.76 Hz ($64 \omega_c$) and is forced by the natural frequency signal at 947.30 Hz, and subharmonic resonance is determined within the magnitude of 0.188 m/s^2 . Other resonance failures are found at the third and fourth dominant peak in frequencies of 866.70 Hz and 947.30 Hz. Vibration on 860.72 Hz which is a harmonic of the cage frequency ($58 \omega_c$) forced a signal at 866.70 Hz as a natural frequency and eventually superharmonic resonance appeared. Vibration on harmonic $2 \times$ is found as the fifth dominant signal on 78.13 Hz. The total sum of the five dominant peaks is 1.483 m/s^2 .

As evaluated in Fig. 2 and Table 3, it is found in axial direction that oil starvation failure induced the vibration intensity of signals at element pass interval.

In radial (vertical) position, vibration at 860.72 Hz is a harmonic of cage frequency ($58 \cdot \omega_c$) forced a vibration magnitude on 866.70 Hz that is a natural frequency and superharmonic resonance is detected within the highest intensity as 0.613 m/s^2 . In radial direction, imbalance harmonic $1 \times$ is found as a second dominant magnitude. Another resonance phenomena are explored at the fourth and fifth dominant magnitudes at frequencies of 948.50 Hz and 120.80 Hz. The vibration magnitude in harmonic of cage failure frequency at 949.76 Hz ($64 \cdot \omega_c$) forced the natural frequency on 948.50 Hz and resonance of subharmonic occurred within intensity of 0.314 m/s^2 . Vibration on 117.18 Hz ($3 \times$) forced the natural frequency on 120.80 Hz and resonance of superharmonic is explored with intensity of 0.277 m/s^2 . Vibration on harmonic $2 \times$ is detected as third dominant signal. Total sum of the five dominant amplitudes is 1.924 m/s^2 .

Table 3. Harmonic indicators of dominant vibrations in axial direction (S – signal).

Measurement (axial)	1.S	2.S	3.S	4.S	5.S
Oil starving	$f_n (3 \times)$	$1 \times$	$f_n (64 \cdot \omega_c)$	$f_n (64 \cdot \omega_c)$	$f_n (2 \times)$

Table 4. Harmonic indicators of dominant vibrations in the radial direction (S – signal).

Measurement (radial)	1.S	2.S	3.S	4.S	5.S
Oil starving	$f_n (58 \cdot \omega_c)$	1×	2×	$f_n (64 \cdot \omega_c)$	$f_n (3 \times)$

According to Fig. 3 and Table 4, in the radial direction, failure of oil starvation induces the vibration amplitude of signals on the element pass frequency interval.

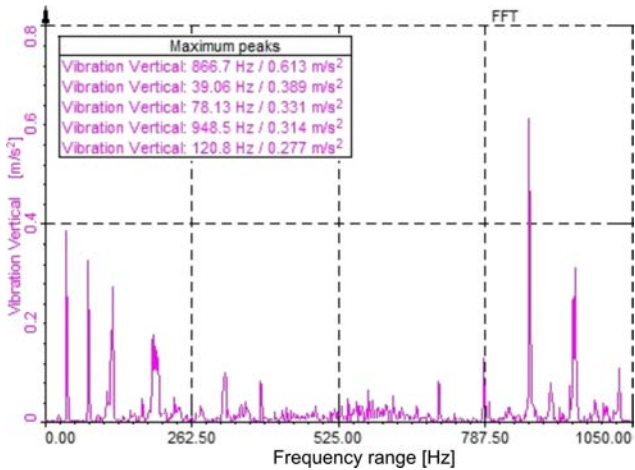


Fig. 3. Spectral view of vibration frequencies (radial direction).

3.3. Electrical consumption analysis

In Fig. 4, electrical consumption values are transformed into standard deviations; the data are based on the trend and PSD analyses. The standard deviation values based on current and voltage variances are given in PSD data and trend data with respect to algorithm of the relevant device software. According to the analysis of PSD in Fig. 4, signal magnitudes

could be identified on harmonics of 40.5 Hz. The greatest three PSD magnitudes were detected on 40.5 Hz, 81 Hz, and 121.5 Hz. According to the systematic algorithm of MCM software, zone of the base frequency indicates the rotor health, zone of the second order indicates the bearing condition and the third order zone indicates other possible faults. Rotor and bearing require care and evaluation with respect to the PSD analysis.

In Fig. 4 an analysis of the trend data, the bearing indicator shows variation in condition of bearing caused by an oil starvation fault.

4. Results and discussion

Within the present study, oil starvation failure happening to a ball bearing and resonance failures have been explored using a test rig system designed uniquely for prognostics and diagnostic testing of mechanical failures. Acoustics, electrical consumption, and vibration technique are implemented in order to investigate the prognostic level of mechanical failures.

To analyze the impact of acoustic technique on effect of oil starvation fault, resonance frequencies and bearing frequencies are checked in the acoustic data.

According to vibration technique evaluations, resonance and bearing fault frequencies are inspected in the spectrum domain by influence of oil starvation fault. Similar frequencies are observed in the axial and radial directions. In relevance with dominance of bearing frequencies, signals in the radial direction can be considered more eminent for determining oil star-

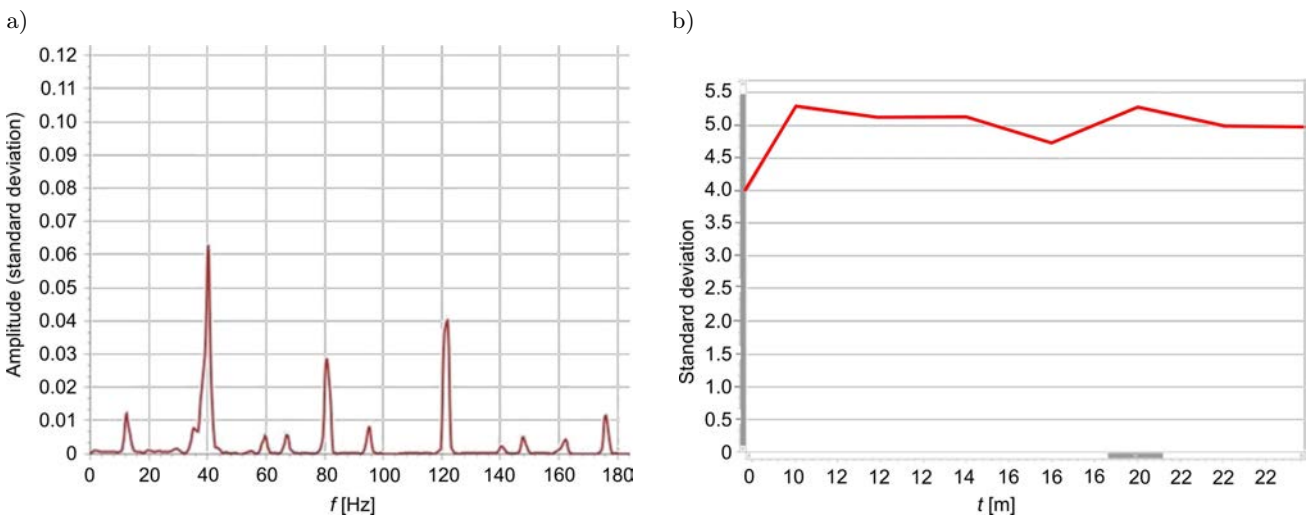


Fig. 4. Electrical consumption data: a) PSD data, b) trend data.

vation. Total magnitude sum of the signals in the radial direction is higher than in the axial direction as well, which means that a higher energy emission has place in the radial direction under the test conditions.

Analysis of electrical consumption is accomplished through diagnosis of oil starving fault in PSD and trend analysis. On the other hand, it is detected that an analysis program of the measuring device is not designed for detection of resonance. But the resonance effect may be studied in the band of rotor; there are no sufficient amount of data about this.

With respect to the analysis of vibration, acoustics and electrical consumption data, vibration technique has been most effective and accurate tool in order to inspect oil starvation fault under resonance phenomenon on the test rig system.

Experimental findings of this research may vary with respect to the internal and external conditions.

5. Conclusions

Condition monitoring technologies mainly base on inspection of the physical indicators belonging to the mechanical systems. In this study, it is concluded that acoustic indicators support the results of vibration analysis in order to inspect oil starvation in the bearing and resonance phenomenon. Electrical consumption indicators support detection of oil starvation by vibration analysis but not the detection of resonance failure.

Amount of resonance quantity and intensity of the degradation may increase and reach catastrophic consequences due to the oil insufficiency. Particular bearing oiling needs may differ with respect to external and internal effects; therefore, oiling needs of a bearing should be checked periodically or predictively, and appropriate lubricating should be carried out continuously.

Detection of resonance phenomena and oil starvation conditions in the prognostic level will lead to taking precautions in order to prevent development in the following stages of the relevant failures.

By means of the developments in signal processing technologies, resonance features of a mechanical structure can be identified in a systematical approach in order to obtain the root cause analysis of subharmonic and superharmonic resonance phenomena.

References

1. ACOSTA G.G., VERUCCHI C.J., GELSO E.R. (2006), A current monitoring system for diagnosing electrical failures in induction motors, *Mechanical Systems and Signal Processing*, **20**(4): 953–965, doi: 10.1016/j.ymsp.2004.10.001.
2. AYO-IMORU R.M., CILLIERS A.C. (2018), A survey of the state of condition-based maintenance (CBM) in the nuclear power industry, *Annals of Nuclear Energy*, **112**: 177–188, doi: 10.1016/j.anucene.2017.10.010.
3. COLLACOTT R.A. (1977), *Mechanical fault diagnosis*, p. 405, Chapman & Hall, London.
4. ER P.V., TAN K.K. (2018), Machine vibration analysis based on experimental modal analysis with radial basis functions, *Measurement*, **128**: 45–54, doi: 10.1016/j.measurement.2018.06.013.
5. EROL S.S. (2016), A Research study on vibrating elements and consuming electricity in predictive maintenance, *European Journal of Interdisciplinary Studies*, **2**(3): 45–50, doi: 10.26417/ejis.v2i3-45-50.
6. GOODENOW T., HARDMAN W., KARCHNAK M. (2000), Acoustic emissions in broadband vibration as an indicator of bearing stress, *IEEE Aerospace Conference Proceedings*, **6**: 95–122, doi: 10.1109/AERO.2000.877886.
7. HARDMAN W., HESS A., SHEAFFER A. (2000), A helicopter powertrain diagnostics and prognostics demonstration, *IEEE Aerospace Conference Proceedings*, **6**: 355–366, doi: 10.1109/AERO.2000.877911.
8. LOUKOPOULOS P. *et al.* (2019), Abrupt fault remaining useful life estimation using measurements from a reciprocating compressor valve failure, *Mechanical Systems and Signal Processing*, **121**: 359–372, doi: 10.1016/j.ymsp.2018.09.033.
9. VELARDE-SUAREZ S., BALLESTEROS-TAJADURA R., HURTADO-CRUZ J.P. (2006), A predictive maintenance procedure using pressure and acceleration signals from a centrifugal fan, *Applied Acoustics*, **67**(1): 49–61, doi: 10.1016/j.apacoust.2005.05.006.
10. WELZ Z., COBLE J., UPADHYAYA B., HINES W. (2017), Maintenance-based prognostics of nuclear plant equipment for long-term operation, *Nuclear Engineering and Technology*, **49**(5): 914–919, doi: 10.1016/j.net.2017.06.001.